Int. J. Heat Mass Transfer. Vol. 14, pp. 1135–1147. Pergamon Press 1971. Printed in Great Britain

THE EFFECT OF FORCED FLOW ON HEAT TRANSFER FROM A DISC ROTATING NEAR A STATOR

J. M. OWEN

School of Applied Sciences, University of Sussex, Falmer, Sussex, England

(*Received* 9 *April* 1970 *and in revised form* 16 *October* 1970)

Abstract—This paper describes the application of the Spalding–Patankar numerical integration procedure to the case of heat transfer from an air-cooled disc rotating close to a stationary casing. Results are calculated to show the effect of frictional heating, arbitrary disc temperature distributions and non-unity Prandtl numbers on heat transfer, and these effects are shown to be qualitatively similar to those predicted by Dorfman for a free disc. Mean Nusselt numbers, calculated for a range of flow parameters, tend to the empirical correlation of Kapinos at high Reynolds numbers but diverge at lower Reynolds numbers. The latter divergence is consistent with the weak dependence of Nusselt number on rotational speed noted by Mitchell and Kreith at low Reynolds numbers.

NOMENCLATURE

A^*, a damping constant in van Driest's turbulence model;

c_0, constant of proportionality in disc temperature distribution;

C_p, specific heat at constant pressure;

C_w, mass flow coefficient, $\equiv W/(\mu r_0)$;

G, gap ratio, $\equiv s/r_0$;

$\bar{h}$, effective total enthalpy, $\equiv C_pT + \frac{1}{2}Pr_{\text{eff}}V_\phi^2$;

$\bar{\bar{h}}$, relative total enthalpy, $\equiv C_pT + \frac{1}{2}Pr_tV_{\phi,\text{rel}}^2$;

h^*, dimensionless enthalpy difference used in wall-flux relations, $\equiv K\,\Delta h(|\tau_{\phi,w}|\rho)^{\frac{1}{2}}/q_w$;

K, mixing-length constant;

l, mixing-length;

n, exponent in disc temperature distribution;

Nu, local Nusselt number, $\equiv q_0r/[\lambda(T_0 - T_{0,\text{ad}})]$;

$\overline{Nu}$, mean Nusselt number, $\equiv q_{0,\text{av}}r/[\lambda(T_0 - T_{0,\text{ad}})_{\text{av}}]$;

p, static pressure;

Pr, Prandtl number;

q, heat flux;

r, r_0, radial coordinate and disc radius, respectively;

Re, Reynolds number, $\equiv \rho\omega^2r_0/\mu$;

R_ϕ^*, local Reynolds number used in wall-flux relations, $\equiv \rho V_{\phi,\text{rel}}z_{\phi,\text{rel}}K^2/\mu$;

s, s_c, axial clearance between rotor and stator, and rotor and shroud, respectively;

S_h^*, dimensionless heat flux used in wall-flux relations, $\equiv q_w/(K^2\rho V_{\phi,\text{rel}}\,\Delta h)$;

S_ϕ^*, dimensionless tangential shear stress used in wall-flux relations, $\equiv \tau_{\phi,w}/(K^2\rho V_{\phi,\text{rel}}^2)$;

T, temperature;

V_r, V_ϕ, V_z, radial, tangential and axial velocity components, respectively;

$\overline{V_r}$, mean radial velocity, $\equiv W/(2\pi\rho rs)$;

W, superimposed mass flow rate;

y_l, a mixing-length constant;

z, axial coordinate measured normal to the rotor;
z_ϕ^*, dimensionless distance from wall used in wall-flux relations, $\equiv Kz_{rel}(|\tau_{\phi,w}|\rho)^{\frac{1}{2}}/\mu$;
α, a mixing-length constant;
ξ, streamwise coordinate;
η, cross-stream coordinate, $\equiv \psi/\bar{\psi}$;
λ, thermal conductivity;
μ, viscosity;
ρ, density;
τ, shear stress;
ψ, stream function;
$\bar{\psi}$, integrated stream function, $\equiv W/2\pi$;
ω, angular velocity of rotating disc.

Suffixes

ad, adiabatic;
av, average;
eff, effective, in turbulent flow;
0, pertaining to the rotor;
r, ϕ, z, radial, tangential and axial directions, respectively;
rel, relative to rotor or stator;
s, pertaining to the stator;
t, turbulent condition;
w, pertaining to wall, rotor or stator.

1. INTRODUCTION

THE CONTINUING development of the gas turbine engine has led to a steady increase in cycle temperatures with the consequent use of cooling air to maintain exposed components at reasonable temperature levels. Effective cooling of the turbine discs—where high pressure air is used to remove heat conducted from the turbine blades and to seal the rotor periphery, thus preventing the ingress of hot gas over the disc faces—poses many design problems. In order to utilize the limited supply of coolant to its full advantage, it is necessary to understand the basic process that controls heat transfer in this highly complicated three-dimensional rotating system.

A fundamental study of a real turbine rotor system would, at the present time, be impracticable owing to the complex geometry of the flow system. However, considerable information can be elicited from the model of a disc rotating near a stationary casing. A large amount of data exists for the free disc, Fig. 1a, and Dorfman [1] has produced procedures for calculating Nusselt numbers on free discs with arbitrary temperature distributions and arbitrary Prandtl numbers.

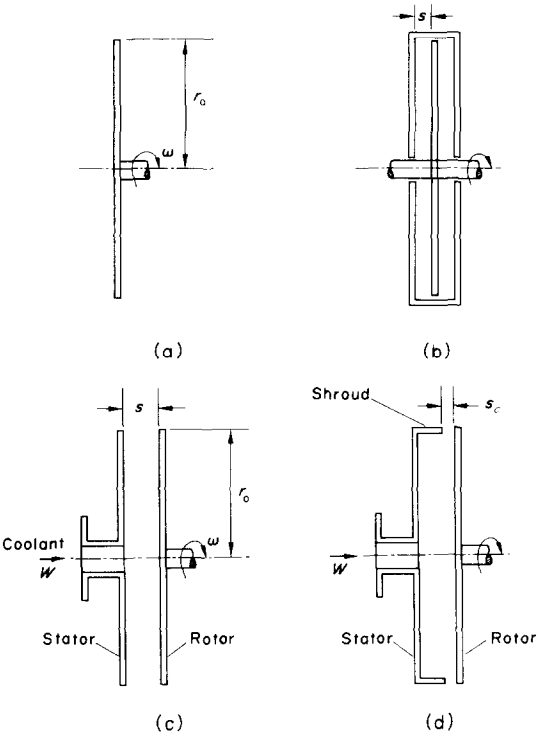

FIG. 1a. Free disc. b. Enclosed disc.
c. Disc rotating near an unshrouded stator.
d. Disc rotating near a shrouded stator.

The present author [2] has shown the conditions necessary for the Reynolds analogy to apply to incompressible and compressible flows, when frictional heating is significant, for free and enclosed discs, Fig. 1b. For the case of a disc rotating near an unshrouded stator with an outflow of coolant, Fig. 1c, Kapinos [3] has produced an analysis of the latter model based

on the Reynolds analogy, but the validity of this technique demands particular boundary conditions which do not, in general, occur in gas turbines. Also, the results of Kapinos are not in accord with the experimental findings of Kreith *et al.* [4] and Mitchell [5].

The fluid dynamics of the disc rotating near an unshrouded stator, [6] Fig. 1c, and a shrouded stator, [7] Fig. 1d, have been investigated by Bayley and Owen. The shrouded system is closer to an air-cooled gas turbine rotor where a peripheral shroud is used to control the egress of coolant and to prevent the ingress of hot gas. In this paper attention is focussed on the unshrouded system, and the analysis of the fluid dynamics of [6] is extended to include heat transfer for the case of a forced radial outflow of coolant. It is believed that knowledge of this relatively simple model will serve as a foundation to the understanding of the more complex practical systems.

2. THE BOUNDARY LAYER EQUATIONS

2.1. *The basic equations*

Expressed in cylindrical polar coordinates for a steady, incompressible, axi-symmetric flow, the radial and tangential momentum equations can be written [1]

$$\rho\left(V_r\frac{\partial V_r}{\partial r}+V_z\frac{\partial V_r}{\partial z}-\frac{V_\phi^2}{r}\right)=-\frac{\mathrm{d}p}{\mathrm{d}r}+\frac{\partial \tau_r}{\partial z} \tag{1}$$

$$\rho\left(V_r\frac{\partial V_\phi}{\partial r}+V_z\frac{\partial V_\phi}{\partial z}+\frac{V_\phi V_r}{r}\right)=\frac{\partial \tau_\phi}{\partial z} \tag{2}$$

where V_r, V_ϕ and V_z are the velocity components in the radial, tangential and axial directions, respectively, p is the static pressure and ρ is the fluid density. For turbulent flow the equations are valid if time-average values are used, and the radial and tangential shear stress components, τ_r and τ_ϕ, respectively, are given by

$$\tau_r=\mu\frac{\partial V_r}{\partial z}-\rho\overline{V_r'V_z'} \tag{3}$$

and

$$\tau_\phi=\mu\frac{\partial V_\phi}{\partial z}-\rho\overline{V_\phi'V_z'} \tag{4}$$

where μ is the fluid viscosity. For laminar flow the velocity fluctuations, represented by primes in equations (3) and (4), vanish.

The continuity equation can be written

$$\frac{1}{r}\frac{\partial}{\partial r}(rV_r)+\frac{\partial V_z}{\partial z}=0, \tag{5}$$

and the energy equation can be expressed as

$$\rho C_p\left(V_r\frac{\partial T}{\partial r}+V_z\frac{\partial T}{\partial z}\right)=-\frac{\partial q}{\partial z}+\tau_r\frac{\partial V_r}{\partial z}+\tau_\phi\frac{\partial V_\phi}{\partial z}, \tag{6}$$

where C_p is the specific heat at constant pressure and T the temperature. The heat flux, q, is related to the temperature by

$$q=-\left(\lambda\frac{\partial T}{\partial z}-\rho\overline{C_pT'V_z'}\right) \tag{7}$$

where λ is the thermal conductivity of the fluid, and the turbulence terms are zero for laminar flow.

2.2. *The effective viscosity model*

A two-component effective viscosity model has been used to good effect in the prediction of the fluid dynamics for this flow system, see [6]. The Prandtl mixing-length theory was employed in its simplest form where:

$$\mu_{r,\mathrm{eff}}=\mu+\mu_{r,t}=\mu+\rho l^2\left|\frac{\partial V_r}{\partial z}\right| \tag{8}$$

and

$$\mu_{\phi,\mathrm{eff}}=\mu+\mu_{\phi,t}=\mu+\rho l^2\left|\frac{\partial V_\phi}{\partial z}\right|. \tag{9}$$

The shear stresses were given by:

$$\tau_r=\mu_{r,\mathrm{eff}}\frac{\partial V_\phi}{\partial z}\quad\text{and}\quad\tau_\phi=\mu_{\phi,\mathrm{eff}}\frac{\partial V_\phi}{\partial z}. \tag{10}$$

A simple ramp distribution of the mixing-length l was assumed such that:

$$\left.\begin{aligned} 0 < z \leqslant \alpha y_l/K: \quad & l = Kz \\ \alpha y_l/K \leqslant z \leqslant s - \alpha y_l/K: \quad & l = \alpha y_l \\ s - \alpha y_l/K \leqslant z < s: \quad & l = K(s - z) \end{aligned}\right\} \quad (11)$$

where s is the distance between the rotating disc and the stator.

The constants α, y_l and K were varied over a range of values, and it was found that $\alpha = 0{\cdot}12$, $y_l = s/2$, and $K = 0{\cdot}4$ gave the best prediction of moment coefficient and pressure distribution. The same constants will be used for the heat-transfer calculations.

Near the rotating disc and the stator the mixing-length is assumed to decay exponentially according to van Driest's hypothesis [10]. The two-component effective viscosity model enables use to be made of the wall flux relations of Patankar and Spalding [8] for the wall shear stresses and, as will be shown later, the wall heat flux. It is now proposed to introduce an effective conductivity, λ_{eff}, where

$$q = -\lambda_{\text{eff}} \frac{\partial T}{\partial z} \quad (12)$$

and

$$\lambda_{\text{eff}} \equiv \left(\lambda \frac{\partial T}{\partial z} - \rho C_p T' V_z'\right) \Big/ \frac{\partial T}{\partial z}. \quad (13)$$

[2] shows that a strong correlation exists between equations (2) and (6), and as a consequence heat transfer is strongly related to the tangential shear stress. It is therefore proposed that—just as for laminar flow (where $\lambda = \mu C_p/Pr$)—the effective conductivity can be expressed as:

$$\frac{\lambda_{\text{eff}}}{C_p} = \frac{\mu_{\phi,\text{eff}}}{Pr_{\text{eff}}} = \frac{\mu}{Pr} + \frac{\mu_{\phi,t}}{Pr_t}. \quad (14)$$

For fully developed turbulent flow $Pr_{\text{eff}} \to Pr_t$. Kestin and Richardson [9], in their comprehensive review of heat transfer in turbulent boundary layers, suggest that whilst experimental measurements of Pr_t through a boundary layer are inconclusive, a constant value can be used as a reasonable approximation. In the majority of the following calculations the turbulent Prandtl number is taken as unity, although the effect of non-unity values of Pr_t is discussed.

2.3. *The transformed equations*

It is convenient to transform the boundary layer equations from r, z coordinates to ξ, ψ coordinates using the von Mises transformation where:

$$V_r = \frac{1}{\rho r}\frac{\partial \psi}{\partial z}, \quad V_z = -\frac{1}{\rho r}\frac{\partial \psi}{\partial r} \quad \text{and} \quad \xi \equiv r.$$

Equations (1), (2) and (6) can now be written

$$\frac{\partial V_r}{\mathrm{d}\xi} = -\frac{1}{\rho V_r}\frac{\mathrm{d}p}{\mathrm{d}\xi} + r\frac{\partial \tau_r}{\partial \psi} + \frac{V_\phi^2}{rV_r} \quad (15)$$

$$\frac{\partial V_\phi}{\partial \xi} = r\frac{\partial \tau_\phi}{\partial \psi} - \frac{V_\phi}{r} \quad (16)$$

$$C_p \frac{\partial T}{\partial \xi} = r\left[-\frac{\partial q}{\partial \psi} + \tau_r \frac{\partial V_r}{\partial \psi} + \tau_\phi \frac{\partial V_\phi}{\partial \psi}\right]. \quad (17)$$

Using equations (15) and (16), equation (17) can be rewritten as

$$\frac{\partial}{\partial \xi}\left(C_p T + \tfrac{1}{2}V_r^2 + \tfrac{1}{2}V_\phi^2 + \frac{p}{\rho}\right) = r\frac{\partial}{\partial \psi}(-q + V_r\tau_r + V_\phi\tau_\phi). \quad (18)$$

Equation (18) can be simplified if the radial terms are negligible. Close to the rotating disc, where frictional effects can be significant, $V_\phi \gg V_r$ and $\tau_\phi \gg \tau_r$. It was shown in [6] that the pressure distribution was, for most cases of interest, more strongly affected by the mass flow rate, W, than by the rotational speed, thus

$$-\frac{1}{\rho}\frac{\mathrm{d}p}{\mathrm{d}r} = 0\left(\overline{V}_r \frac{\mathrm{d}\overline{V}_r}{\mathrm{d}r}\right) \text{where } \overline{V}_r = W/(2\pi\rho rs).$$

If the radial velocity is relatively small, as is the case for air-cooled turbine rotors, the terms

$$\frac{\partial}{\partial \xi}\left(\tfrac{1}{2}V_r^2 + \frac{p}{\rho}\right) \quad \text{and} \quad r\frac{\partial}{\partial \psi}(V_r \tau_r)$$

can be neglected in comparison with the other terms. Under these conditions equation (18) can be simplified by introducing the new variables

$$h \equiv C_p T + \tfrac{1}{2} Pr_{\text{eff}} V_\phi^2 \tag{19}$$

and

$$\eta \equiv \psi/\bar{\psi} \tag{20}$$

where

$$\bar{\psi} = \int_0^s \frac{\partial \psi}{\partial z}\,\mathrm{d}z = W/2\pi. \tag{21}$$

Hence from these definitions, and using the effective viscosity model, equation (18) becomes

$$\frac{\partial \bar{h}}{\partial \xi} = \frac{\rho r^2}{\bar{\psi}^2}\frac{\partial}{\partial \eta}\left[V_r \frac{\mu_{\phi,\text{eff}}}{Pr_{\text{eff}}}\frac{\partial \bar{h}}{\partial \eta}\right] - (1 - Pr_{\text{eff}})\, V_\phi \frac{\partial V_\phi}{\partial \xi}. \tag{22}$$

Similarly, using equation (20) and the effective viscosity models, equations (15) and (16) can be rewritten as

$$\frac{\partial V_r}{\partial \xi} = \frac{\rho r^2}{\bar{\psi}^2}\frac{\partial}{\partial \eta}\left(V_r \mu_{r,\text{eff}}\frac{\partial V_r}{\partial \eta}\right) - \frac{1}{\rho V_r}\frac{\mathrm{d}p}{\mathrm{d}\xi} + \frac{V_\phi^2}{rV_r} \tag{23}$$

$$\frac{\partial}{\partial \xi}(rV_\phi) = \frac{\rho r^2}{\bar{\psi}^2}\frac{\partial}{\partial \eta}\left(V_r \mu_{\phi,\text{eff}}\frac{\partial V_\phi}{\partial \eta}\right). \tag{24}$$

Equations (22)–(24) are the equations that will be solved numerically.

2.4. *The Reynolds analogy*

For the case of $Pr = Pr_t = Pr_{\text{eff}} = 1$, the analogy between equations (22) and (24) is complete if the initial and boundary conditions are similar. For a quadratic temperature rise over the rotating disc radius and for an isothermal stator the boundary conditions become

$$\eta = 0: rV_{\phi,0} = \omega r^2, \qquad \bar{h}_0 = c_0 r^2$$

$$\eta = 1: rV_{\phi,s} = 0, \qquad \bar{h}_s = \text{constant}$$

where the subscripts 0 and s refer to the rotor and stator, respectively, and c_0 is a constant. Under these conditions the distribution of tangential velocity and enthalpy are similar, hence

$$\frac{\bar{h} - \bar{h}_s}{\bar{h}_0 - \bar{h}_s} = \frac{V_\phi}{\omega r} \tag{25}$$

and as

$$q = -\mu_{\phi,\text{eff}}\frac{\partial}{\partial z}(\bar{h} - \tfrac{1}{2}V_\phi^2) \tag{26}$$

it follows from equation (25) that

$$q = V_\phi \tau_\phi - \frac{\bar{h}_0 - \bar{h}_s}{\omega r} \tag{27}$$

thus

$$q_0 = -\frac{\tau_{\phi,0}}{\omega r}[C_p(T_0 - T_s) - \tfrac{1}{2}\omega^2 r^2]. \tag{28}$$

For an adiabatic disc, $q_0 = 0$, and

$$T_{0,\text{ad}} = T_s + \tfrac{1}{2}\omega^2 r^2 / C_p \tag{29}$$

which agrees with the result obtained in [2] despite the fact that the radial dissipation has been ignored in the present case. It would therefore appear that the neglect of radial effects should not reduce the generality of the solution procedure.

3. NUMERICAL SOLUTION OF THE BOUNDARY LAYER EQUATIONS

3.1. *The numerical method*

The techniques used to solve equations (22)–(24) are an extension of the method employed to solve the momentum equations in (6). The fluid dynamics predictions had been compared with results from an experimental rig at the University of Sussex where a 30 in. dia. disc was rotated up to 4500 rpm close to a stator of the same diameter. In those calculations it was found that 50 radial steps, from

$r/r_0 = 0{\cdot}32$ to $r/r_0 = 1$, and up to 120 cross-stream steps, for gap ratios up to $G = 0{\cdot}12$ (where $G \equiv s/r_9$), were necessary in order to achieve a satisfactory momentum balance. Initial distributions of radial velocity were based upon a $\frac{1}{7}$th power law pipe flow, and the tangential velocity distribution decayed from ωr on the disc to zero on the stator according to a $\frac{1}{7}$th power law. For the calculation of heat transfer, the distribution of enthalpy was assumed to be similar to the distribution of tangential velocity at the starting radius. The implicit finite-difference method used, that of Spalding and Patankar, [8] could be made more efficient by the use of wall flux relations obtained from the solution of the ordinary differential equations resulting from the Couette flow close to a wall. Just as it had been necessary to modify these relations close to a rotating disc for the fluid dynamics problem, so it was found necessary to make allowances for rotation in the heat transfer problem.

3.2. *Calculation of the wall fluxes*

Near an impermeable wall, either the stator or the rotating disc, use is made of the van Driest hypothesis [10] for the effective viscosity in equation (9) and it is assumed that

$$\mu_{\phi,\mathrm{eff}}/\mu = 1 + z_\phi^{*2}[1 - \exp(-z_\phi^*\sqrt{\tau_\phi^*}/A^*)]^2 \times |\partial V_\phi^*/\partial z_\phi^*| \qquad (30)$$

where

$$z_\phi^* = K z_{\mathrm{rel}}(|\tau_{\phi,w}|)^{\frac{1}{2}}/\mu \qquad (31a)$$

$$\tau_\phi^* = \tau_\phi/\tau_{\phi,w} \qquad (31b)$$

$$V_\phi^* = K V_{\phi,\mathrm{rel}}/(\tau_{\phi,w}/\rho)^{\frac{1}{2}}. \qquad (31c)$$

The subscript w is used to refer to the wall, either rotor or stator, and z_{rel} and $V_{\phi,\mathrm{rel}}$ are the distance and velocity, respectively, relative to that wall. $V_{\phi,\mathrm{rel}} = V_\phi - \omega r$, $z_{\mathrm{rel}} = z$ near the rotor, and $V_{\phi,\mathrm{rel}} = V_\phi - \omega r$, $z_{\mathrm{rel}} = s - z$ near the stator. K is a mixing-length constant, and A^* is a damping constant. From equation (2) it is apparent that the convection terms tend to zero near the rotor and the stator, and so close to the rotating disc, in the so-called Couette flow region, the tangential shear stress tends to the wall value, such that $\tau_\phi = \tau_{\phi,0}$. Similarly on the stator, $\tau_\phi = \tau_{\phi,s}$, and so for rotor or stator

$$\tau_\phi^* = \frac{\mu_{\phi,\mathrm{eff}}}{\mu}\frac{\mathrm{d}V_\phi^*}{\mathrm{d}z_\phi^*} = 1. \qquad (32)$$

Substituting equation (32) into equation (31) produces

$$\frac{\mathrm{d}V_\phi^*}{\mathrm{d}z_\phi^*} = \frac{2}{1 + \{1 + 4z_\phi^{*2}[1 - \exp(-z_\phi^*/A^*)]^2\}^{\frac{1}{2}}}. \qquad (33)$$

Numerical solutions to equation (33) can be found in [8] and the answers express the wall shear stress in terms of the local Reynolds number such that:

$$S_\phi^* \equiv \tau_{\phi,w}/(K^2\rho V_{\phi,\mathrm{rel}}^2) = R_\phi^{*-1} - 0{\cdot}1561\,R_\phi^{*-0{\cdot}45} + 0{\cdot}08723\,R_\phi^{*-0{\cdot}3} + 0{\cdot}03713\,R_\phi^{*-0{\cdot}18} \qquad (34)$$

where

$$R_\phi^* \equiv \rho V_{\phi,\mathrm{rel}} z_{\mathrm{rel}} K^2/\mu.$$

For the case of the energy equation, application of the van Driest hypothesis gives the result:

$$\frac{\mu_{\phi,\mathrm{eff}}}{\mu Pr_{\mathrm{eff}}} = \frac{1}{Pr} + \frac{z_\phi^{*2}}{Pr_t} \times \left\{1 - \exp[-z_\phi^*(\sqrt{\tau_\phi^*})/A^*]\right\}^2 \Big/ \frac{\mathrm{d}V_\phi^*}{\mathrm{d}z_\phi^*}. \qquad (35)$$

If, by analogy with equation (32), we can define a new variable h^* such that:

$$\frac{\mu_{\phi,\mathrm{eff}}}{\mu Pr_{\mathrm{eff}}}\frac{\mathrm{d}h^*}{\mathrm{d}z_\phi^*} = 1 \qquad (36)$$

then equations (35) and (36) combine to give:

$$\frac{\mathrm{d}h^*}{\mathrm{d}z_\phi^*} = \frac{Pr_t}{Pr_t/Pr + z_\phi^{*2}[1 - \exp(-z_\phi^*/A^*)]^2(\mathrm{d}V_\phi^*/\mathrm{d}z_\phi^*)}. \qquad (37)$$

The solution to equation (37) is expressed in [8] as

$$S_h^* = \frac{S_\phi^*}{Pr_t[1 + 3{\cdot}68\, S_\phi^{*\frac{1}{2}}(Pr/Pr_t)^{\frac{1}{2}}(Pr/Pr_t - 1)]} \tag{38}$$

where

$$S_h^* \equiv \frac{q_w}{K^2 \rho V_{\phi,\mathrm{rel}}\, \Delta h} \tag{39}$$

and we define h^* as

$$h^* \equiv K\, \Delta h (|\tau_{\phi,w}|\rho)^{\frac{1}{2}}/q_w. \tag{40}$$

It is now necessary to derive an expression for Δh.

3.3. *The motivating temperature difference for heat transfer near a rotating disc*

In the Couette-flow region near the rotor, if the convection terms are small compared with the flux, equation (22) simplifies to:

$$\frac{\partial}{\partial \eta}\left[V_r \frac{\mu_{\phi,\mathrm{eff}}}{Pr_{\mathrm{eff}}} \frac{\partial \bar{h}}{\partial \eta}\right] = 0 \tag{41}$$

which implies that

$$q - \tau_\phi V_\phi = q_0 - \tau_{\phi,0} V_{\phi,0}. \tag{42}$$

For an adiabatic disc $q_0 = 0$, hence

$$q_{\mathrm{ad}} = \tau_{\phi,0} V_{\phi,\mathrm{rel}} \tag{43}$$

where

$$\tau_\phi = \tau_{\phi,0} \quad \text{and} \quad V_{\phi,\mathrm{rel}} = V_\phi - V_{\phi,0},$$

subscript 'ad' referring to the adiabatic condition. Equation (43) can be written as

$$-\frac{\mu_{\phi,\mathrm{eff}}}{Pr_{\mathrm{eff}}} \frac{\partial}{\partial z}(C_p T)_{\mathrm{ad}} = \mu_{\phi,\mathrm{eff}} \frac{\partial V_\phi}{\partial z} V_{\phi,\mathrm{rel}}. \tag{44}$$

Hence

$$C_p(T_{0,\mathrm{ad}} - T_{\mathrm{ad}}) = \int_0^{\frac{1}{2}V_{\phi,\mathrm{rel}}^2} Pr_{\mathrm{eff}}\, \mathrm{d}(\tfrac{1}{2}V_{\phi,\mathrm{rel}}^2), \tag{45}$$

which can be evaluated approximately by noting that Pr_{eff} only deviates significantly from Pr_t in the region where $V_{\phi,\mathrm{rel}}$ is small and the value of the integral is correspondingly small. Thus equation (45) can be approximated by:

$$C_p T_{0,\mathrm{ad}} = C_p T_{\mathrm{ad}} + \tfrac{1}{2} Pr_t V_{\phi,\mathrm{rel}}^2. \tag{46}$$

It is interesting to observe the similarity between equations (46) and (29) for $Pr_t = 1$.

We now define a variable $\bar{\bar{h}}$ such that

$$\bar{\bar{h}} \equiv C_p T + \tfrac{1}{2} Pr_t V_{\phi,\mathrm{rel}}^2, \tag{47}$$

and from equations (42) and (43) it follows that:

$$\frac{\mu_{\phi,\mathrm{eff}}}{Pr_{\mathrm{eff}}} \frac{\mathrm{d}}{\mathrm{d}z}(\bar{\bar{h}}_0 - \bar{\bar{h}}) = q_0. \tag{48}$$

Comparing equations (48) and (36) we see that

$$h^* = K(\bar{\bar{h}}_0 - \bar{\bar{h}})(|\tau_{\phi,0}|\rho)^{\frac{1}{2}}/q_0, \tag{49}$$

or

$$\Delta h = \bar{\bar{h}}_0 - \bar{\bar{h}}. \tag{50}$$

A similar argument applied to the stator, where $V_{\phi,\mathrm{rel}} = V_\phi$, yields

$$\Delta h = \bar{\bar{h}} - \bar{\bar{h}}_s. \tag{51}$$

Using Δh, as calculated from equations (50) or (51), the heat flux through the rotor or stator can be evaluated from the wall flux relation, equation (38).

4. TESTING THE NUMERICAL METHOD

Before comparisons with experimental data can be made it is necessary to check that the Reynolds analogy conditions ($T_0 = c_0 r^2$, $T_s = 0$, $Pr = Pr_t = 1$) should produce similar enthalpy and tangential velocity profiles, and that the wall fluxes should be compatible. For the case of zero dissipation and of finite dissipation these conditions were fully satisfied by the use of h^* given in equation (49). This consistency is a necessary condition for accuracy, but the accuracy of predicted Nusselt numbers can be no greater than the accuracy of the predicted frictional moment coefficients.

As a direct consequence of the Reynolds analogy, the local Nusselt number, Nu, is related to the shear stress by

$$Nu = -\frac{\tau_{\phi,0}}{\mu\omega} \tag{52}$$

where

$$Nu \equiv \frac{q_0 r}{\lambda(T_0 - T_{0,\mathrm{ad}})}. \tag{53}$$

For non-unity Prandtl numbers and arbitrary disc temperatures ($T_0 = c_0 r^n$, n being the arbitrary exponent and c_0 a constant) Dorfman [1] obtained solutions of the integral equations for the free disc and showed that

$$Nu(Pr, n) \doteq Nu(Pr = 1, n = 2) \times Pr^{0.6}\left[\frac{n + 2.6}{4.6}\right]^{0.2}. \tag{54}$$

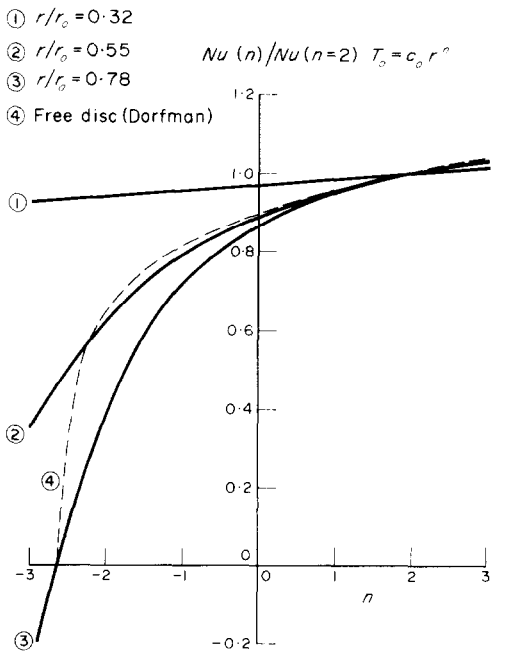

FIG. 2. Effect of disc temperature distribution on local Nusselt numbers for $G = 0{\cdot}03$, $C_w = 2{\cdot}5 \times 10^4$, $Re = 4 \times 10^6$.

For comparison, numerical integration was conducted for the case of a disc rotating near an isothermal stator with a radial outflow for $Pr = 1$ and a range of exponents $-3 \leqslant n \leqslant 3$. As the integration was commenced assuming complete similarity between the initial enthalpy and tangential velocity distributions, any index other than $n = 2$ produced a developing flow condition in which the temperature and velocity distributions became progressively different. The divergence increased with increasing radius, and the rate of divergence varied according to the value of n.

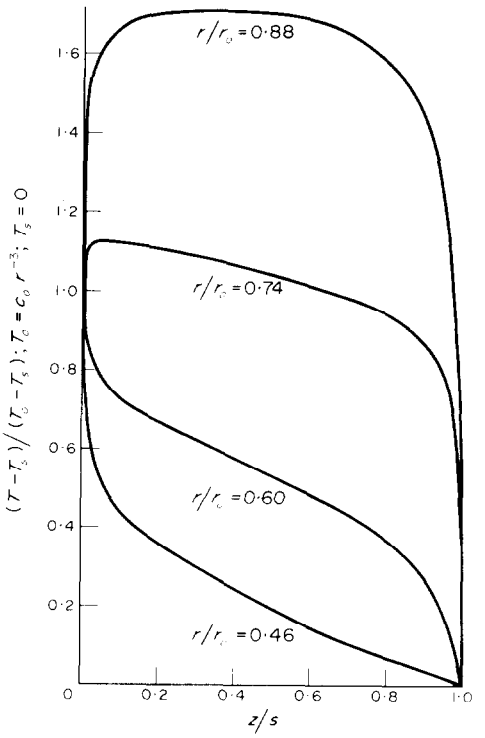

FIG. 3. Effect of radially decreasing disc temperature on axial temperature profiles for $G = 0{\cdot}03$, $C_w = 2{\cdot}5 \times 10^4$, $Re = 4 \times 10^6$.

In the ensuing calculations the turbulent Prandtl number is assumed to be unity, and the axial gap is characterised by a gap ratio, G, and the mass flow rate is described by a mass flow coefficient, $C_w \equiv W/(\mu r_0)$. Figure 2 illustrates the effect of disc temperature distribution on Nusselt number at different radial positions for a starting radius ratio of $r/r_0 = 0{\cdot}3$. The effect of radial position is more evident for negative

values of n, and at a radius ratio of $r/r_0 = 0{\cdot}78$ heat transfer from the rotating disc is prevented for $n < -2{\cdot}6$. The fact that the value equals the critical index in equation (54) is coincidental: the critical index will be smaller for larger radii and vice versa.

Figure 3 shows the developing temperature profiles for $n = -3$ where, in order to show the effect of disc temperature profile without frictional heating complicating the picture, dissipation is neglected. Whilst the temperature gradient at the disc surface is originally favourable for heat transfer from the disc, it gradually becomes smaller and eventually reverses. After reversal heat removed from the disc at the smaller radii is dumped back in at larger radii, the latter effect occuring despite the ostensibly favourable temperature difference between the rotor and stator. It should be noted that frictional heating would accelerate this heat reversal. Whilst negative values of n cannot occur under steady-state operation of gas turbines they can occur when the engine power is reduced and the turbine blades, and hence the disc tip, begin to cool. Under these circumstances, the failure of the coolant to remove heat from the disc tip would help to slow down the blade cooling, and could therefore prove advantageous.

An undesirable situation would occur if heat transfer from the disc were to be reversed during steady-state operation. This could happen if the coolant temperature were not low enough to prevent frictional heating of the rotor. The effect is illustrated in Fig. 4 for an isothermal rotor where, owing to the rapid decay of the tangential velocity near the rotating disc, dissipation terms are only significant very close to the rotor. Although the temperature profile gradually changes with increasing radius, the gradient only reverses in the "Couette-flow" region: outside of this region heat is transferred away from the disc, whilst inside it is transferred into the disc. Disc heating commences at $r/r_0 = 0{\cdot}59$ despite the apparently favourable gradient existing away from the disc surface, and dissipative heat not conducted through the disc itself

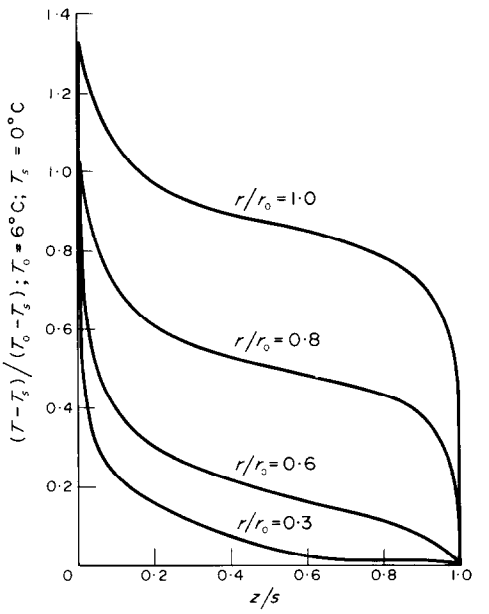

FIG. 4. Effect of frictional heating on axial temperature profiles for $G = 0{\cdot}03$, $C_w = 2{\cdot}5 \times 10^4$, $Re = 4 \times 10^6$.

serves to raise the bulk temperature of the fluid. The effects of heat reversal due to disc temperature distribution and to frictional heating for the case of laminar impinging flow on a free rotating disc have been calculated by Mabuchi *et al.* [11]. The numerical results obtained for the present system are qualitatively similar, but frictional heating is much more local in turbulent flow than in laminar flow owing to the steeper gradients associated with the former case.

The effect of Prandtl number on heat transfer for $T_0 = c_0 r^2$ is illustrated in Fig. 5 by the ratio of $\overline{Nu}(Pr)/\overline{Nu}(Pr = 1)$ for $0{\cdot}5 \leqslant Pr \leqslant 8$, where

$$\overline{Nu} \equiv \frac{q_{0,\,\mathrm{av}}\, r_0}{\lambda (T_0 - T_{0,\,\mathrm{ad}})_{\mathrm{av}}} \tag{55}$$

and

$$q_{0,\,\mathrm{av}} = \frac{2}{r_0^2} \int_0^{r_0} r\, q_0 \, \mathrm{d}r. \tag{56}$$

It can be seen that although the effect of Prandtl number does depend upon the flow

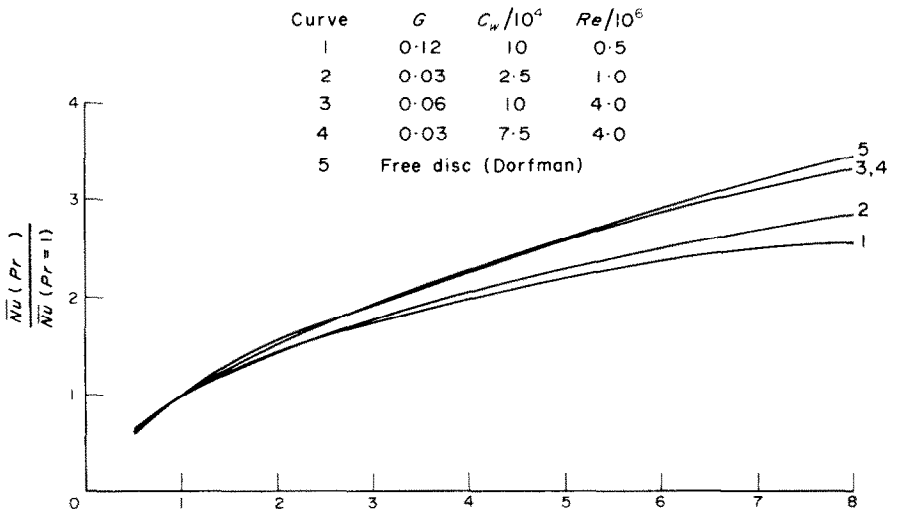

FIG. 5. Calculated effect of Prandtl number on the mean Nusselt number for a range of flow parameters.

characteristics of the system, for gases ($Pr < 1$) Dorfman's correction is a good approximation. For large Prandtl numbers the accuracy of the approximation appears to depend more on Reynolds number than the other parameters. As at large Reynolds numbers the moment coefficients, measured and calculated, for this system tend to those of the free disc, it would appear that application of the free disc correction is more valid for $Re > 10^6$.

It should be pointed out that calculations were carried out for a range of Reynolds numbers with $Pr = 1$, and Pr_t varied between 0·6 and 1. It was observed that for $Pr_t = 0{\cdot}8$ the mean Nusselt number increased by 8 per cent at $Re = 4 \times 10^5$ to 11 per cent at $Re = 4 \times 10^6$, compared with the values for $Pr_t = 1$. A similar increase over the values at $Pr_t = 0{\cdot}8$ was observed for $Pr_t = 0{\cdot}6$. Kestin and Richardson [9] have noted that most heat-transfer theories either assume $Pr_t = 1$, or assume a constant value, say $Pr_t = 0{\cdot}78$, in order to obtain acceptable predictions. No firm recommendation can be made for the present system until more experimental data are available.

The behaviour of the numerical solutions for arbitrary disc temperatures, arbitrary Prandtl numbers, and with frictional heating, is consistent—if not identical— with that found for the free disc. It would therefore appear that the solutions of equation (22) are compatible with free disc calculations, and it remains to verify that the solutions obtained agree with experimental results.

In Fig. 6 the calculated Nusselt numbers are compared with the experimental data of Kapinos[3]. The experiments were conducted on a 645 mm dia. disc, placed at distances of from 88 to 115 mm from a stator, and rotated up to 3500 rpm. The numerical solution shows better agreement at larger gap ratios and larger Reynolds numbers, and the relative increase of Nusselt number with increasing mass flow rate is predicted with reasonable accuracy. At low Reynolds numbers the calculated Nusselt numbers tend to become more dependent on mass flow rate and less dependent on rotational speed. This effect is consistent with the Reynolds analogy [2] applied to the moment coefficients of Bayley and Owen [6], and is in qualitative agreement with the results of Kreith *et al.*[4] and Mitchell [5].

It should also be pointed out that some of the experimental values used for comparison in Fig. 6 were obtained by extrapolating Kapinos' empirical correlation outside of its verified range.

Although no experimental local Nusselt numbers are available for comparison, Fig. 7 shows

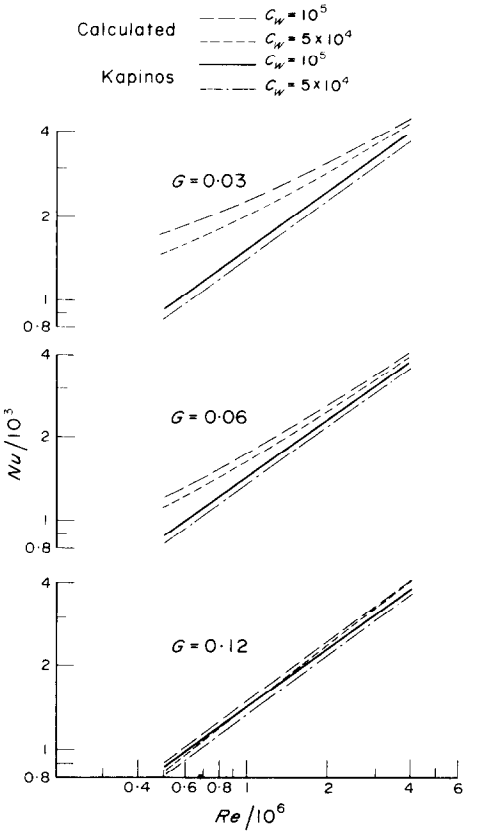

FIG. 6. Comparison of calculated mean Nusselt numbers with the empirical correlation of Kapinos.

numerically calculated results for a gap ratio of $G = 0{\cdot}06$ and a mass flow rate of $C_w = 5 \times 10^4$. The local Nusselt numbers, plotted for a range of Reynolds number, are compared with the free disc result based on the Reynolds analogy applied to von Kármán's calculated moment coefficient where

$$Nu = 0{\cdot}0267\,(r/r_0)^{1{\cdot}6}\,Pr^{0{\cdot}6}\,Re^{0{\cdot}8}. \quad (57)$$

The calculated Nusselt numbers are, as would be expected, larger than the free disc values, although the trends are not significantly different.

Although the results of the numerical method are encouraging, it is apparent that more experimental data are necessary before rigorous tests can be applied to check the quantitative accuracy of the boundary layer model and its method of solution. A programme of research into the heat

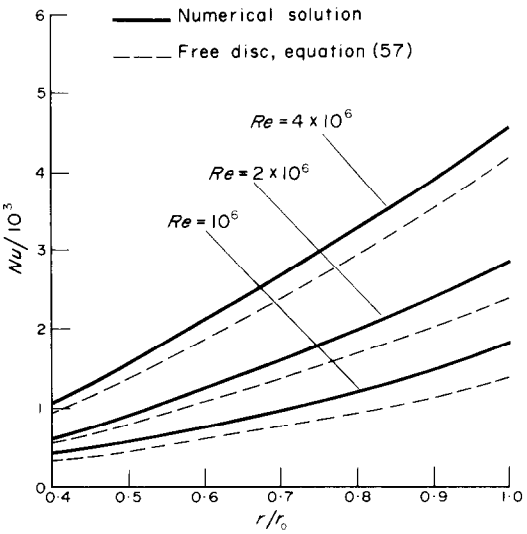

FIG. 7. Local Nusselt numbers for $G = 0{\cdot}06$. $C_w = 5 \times 10^4$, $Pr = 0{\cdot}72$.

transfer from a rotating disc is currently in operation in the Mechanical Engineering Laboratories at the University of Sussex, and it is hoped that future experimental data will provide a useful testing ground for the existing calculation procedure.

CONCLUSIONS

The Spalding–Patanker numerical integration procedure [8] has been applied to heat transfer from a disc rotating near a stator, with a radial outflow of coolant, and the principal conclusions to be drawn are as follows:

(i) For the case of an isothermal stator ($T_s =$

constant) a quadratic temperature distribution over the rotating disc ($T_0 \propto r^2$), and unity Prandtl numbers ($Pr = Pr_t = 1$), the Nusselt numbers calculated by the numerical procedure are in exact agreement with the Reynolds analogy.

(ii) For arbitrary disc temperatures ($T_0 \propto r^n$) the Nusselt number, whilst being radius-dependent, behaves in a manner consistent with Dorfman's free disc result [1]

$$Nu(n) \doteqdot Nu(n = 1)\left[\frac{n + 2{\cdot}6}{4{\cdot}6}\right]^{0{\cdot}2}.$$

(iii) The effect of arbitrary laminar Prandtl numbers (Pr_t assumed unity) on the Nusselt number was found to be dependent on Reynolds number. For $Re > 10^6$, the results can be approximated over the range $0{\cdot}5 < Pr < 2$ by Dorfman's free disc result

$$Nu\,(Pr) \doteqdot Pr^{0{\cdot}6}\, Nu(Pr = 1).$$

(iv) Frictional heating due to tangential dissipation was included in the solution procedure, and the effects of this are qualitatively similar to the predictions of Mabuchi *et al.* [11] for forced laminar flow over a free disc.

(v) For high values of Reynolds numbers ($Re > 10^6$) the calculated mean Nusselt numbers tend to the experimental results of Kapinos [3]. At low Reynolds numbers, and at the smaller gap ratios ($G < 0{\cdot}06$), the calculated Nusselt numbers show more dependence on mass flow rate, C_w, and less dependence on Re than the results of Kapinos. The calculated results at low Reynolds numbers are therefore qualitatively similar to the experimental findings of Mitchell [5] and Kreith *et al.* [4].

(vi) Although no experimental values of local Nusselt number are currently available, the calculated values show that the effect of forced flow is to increase the local heat-transfer rate compared with that of a free disc. The relative increase will, however, depend on the gap ratio, the mass flow rate and the rotational speed or the system under consideration.

ACKNOWLEDGEMENTS

The author wishes to acknowledge Rolls-Royce Limited for their continuing support of this work, and to thank Professor F. J. Bayley for his advice and encouragement.

REFERENCES

1. L. A. Dorfman, *Hydrodynamic Resistance and Heat Loss of Rotating Solids*. Oliver & Boyd, Edinburgh (1963).
2. J. M. Owen, The Reynolds analogy applied to flow between a rotating and a stationary disc, *Int. J. Heat Mass Transfer* **14**, 451–460 (1971).
3. V. M. Kapinos, Heat transfer from a disc rotating in a housing with a radial flow of coolant, *J. Engng Phys.* **8**, 35 (1965).
4. F. Kreith, E. Doughman and H. Kozlowski, Mass and heat transfer from an enclosed rotating disc with and without source flow, *J. Heat Transfer* **85**, 153 (1963).
5. J. W. Mitchell, A study of the fluid dynamics and heat transfer behaviour for radially inward flow over a shrouded rotating disc, TR No. 57. Dept. Mech. Engng, Stanford University (1963).
6. F. J. Bayley and J. M. Owen, Flow between a rotating and a stationary disc, *Aeronaut. Q.* **20**, 333 (1969).
7. F. J. Bayley and J. M. Owen, The fluid dynamics of a shrouded disc system with a radial outflow of coolant, *J. Engng Pwr* **92**, 335 (1970).
8. D. B. Spalding and S. V. Patankar, *Heat and Mass Transfer in Boundary Layers*. Morgan-Grampian, London (1967).
9. J. Kestin and P. D. Richardson, Heat transfer across turbulent incompressible boundary layers, *Int. J. Heat Mass Transfer* **6**, 147 (1963).
10. E. R. Van Driest, On turbulent flow near a wall, *J. Aeronaut. Sci.* **23**, 1007 (1956).
11. I. Mabuchi, T. Tanaka and Y. Sakakibara, Studies on the convective heat transfer from a rotating disc, *Bull. JSME* **10**, 104 (1967).

EFFET D'UN ÉCOULEMENT FORCÉ SUR LE TRANSFERT THERMIQUE DEPUIS UN DISQUE TOURNANT PRÈS D'UN STATOR

Résumé—Cet article décrit l'application de la méthode d'intégration numérique de Spalding-Patankar au cas du transfert thermique depuis un disque tournant refroidi par air, proche d'une enceinte stationnaire.

Les calculs sont conduits afin de montrer l'effet sur le transfert thermique de l'échauffement par frottement des distributions arbitraires de température du disque et des nombres de Prandtl non unitaires. On montre que ces effets sont qualitativement similaires à ceux prédits par Dorfman pour un disque libre. Des nombres de Nusselt moyens, calculés pour un domaine de paramètres d'écoulement, tendent vers la formule empirique de Kapinos pour des grands nombres de Reynolds mais divergent pour des plus petits nombres de Reynolds. Cette divergence est en relation avec la faible dépendance du nombre de Nusselt à la vitesse rotationnelle notée par Mitchell et Kreith pour des petits nombres de Reynolds.

DER EINFLUSS VON ERZWUNGENER STRÖMUNG AUF DEN WÄRMEÜBERGANG AN EINER SCHEIBE, DIE NAHE EINES STATORS ROTIERT

Zusammenfassung—Die Arbeit beschreibt die Anwendung der numerischen Integrationsprozedur nach Spalding–Patankar auf den Wärmeübergang an einer luftgekühlten Scheibe, die nahe eines feststehenden Gehäuses rotiert. Die Rechenergebnisse zeigen den Einfluss von Aufheizung durch Reibung, von beliebigen Scheibentemperaturverteilungen und von Prandtl-Zahlen $\neq 1$ auf den Wärmeübergang. Es zeigt sich, dass diese Einflüsse jenen qualitativ ähnlich sind, die von Dorfman für die freie Scheibe vorausgesagt wurden. Mittlere Nusselt-Zahlen, die für eine Reihe von Strömungsparametern berechnet wurden, stimmen mit der empirischen Korrelationsformel von Kapinos für grosse Reynoldszahlen überein, weichen jedoch bei kleinen Reynoldszahlen davon ab. Diese Abweichung steht in Einklang mit der schwachenAbhängigkeit der Nusselt-Zahl von der Winkelgeschwindigkeit bei kleinen Renolds-Zahlen, wie sie von Mitchell und Kreith gefunden wurde.

ВЛИЯНИЕ ВЫНУЖДЕННОГО ТЕЧЕНИЯ НА ПЕРЕНОС ТЕПЛА ОТ ДИСКА, ВРАЩАЮЩЕГОСЯ ВОЗЛЕ СТАТОРА

Аннотация—В статье описывается применение метода численного интегрирования Сполдинга-Патанкара для случая переноса тепла от охлаждаемого воздухом диска, вращающегося возле стационарной стенки. Приводятся расчёты, для того чтобы показать влияние на теплообмен аэродинамического нагрева, произвольного распределения температуры диска и отклонения числа Прандтля от единицы. Кроме того показано, что эти эффекты качественно согласуются с результатами расчёта Дорфмана для свободного диска. Средние числа Нуссельта, рассчитанные для какого-то диапазона параметров, приближаются к эмпирическим соотношениям Капиноса при больших числах Рейнольдса, но отклоняются от них при малых числах Рейнольдса. Это различие связано со слабой зависимостью числа Нуссельта от скорости вращения, замеченной Митчеллом и Крейсом при малых числах Рейнольдса.